Imaging and Treatment of B-Cell Lymphoma

Janet F. Eary, Oliver W. Press, Christopher C. Badger, Lawrence D. Durack, Karen Y. Richter, Stanley J. Addison, Kenneth A. Krohn, Darrell R. Fisher, Bruce A. Porter, David L. Williams, Paul J. Martin, Frederick R. Appelbaum, Ronald Levy, Sherri L. Brown, Richard A. Miller, Wil B. Nelp, and Irwin D. Bernstein

Departments of Radiology, Division of Nuclear Medicine, Medicine and Pediatrics, University of Washington Medical Center; Fred Hutchinson Cancer Research Center, First Hill Diagnostic Inc., Seattle, Washington; Battelle Pacific Northwest Laboratories, Richland, Washington; Department of Medicine, Stanford University, Stanford, California; and IDEC Pharmaceuticals Corp., Mountain View, California

Ten patients with non-Hodgkin's lymphoma have been evaluated as candidates for experimental radioimmunotherapy and five of those patients have been treated with a single high dose of iodine-131- (^{131}I) labeled anti-pan B-cell antibodies. The evaluation protocol involved collecting biodistribution data by quantitation of gamma camera images and by tumor biopsy from trace labeled doses of antibody, to estimate the relative radiation dose delivered to normal organs and tumor sites. Each patient received up to three escalating mass doses (0.5 mg/kg, 2.5 mg/kg, and 10.0 mg/kg) of radioiodinated antibody for determination of the antibody amount that yielded the most favorable biodistribution for treatment. The millicuries of ^{131}I-labeled to the optimal antibody dose for therapy was selected to deliver 1,000 rads (three patients) or 1,500 rads (two patients) to normal uninvolved organs. Because severe bone marrow toxicity was expected, all patients had their bone marrow cryopreserved prior to entry into the study. This report details the methods and results of quantitative imaging, biodistribution data collection, and absorbed radiation dose estimation in patients with lymphoma receiving high level radioimmunotherapy with ^{131}I-labeled antibodies.

J Nucl Med 1990; 31:1257–1268

Effective radioimmunotherapy of cancer has been a goal of many research groups for several years (*1–5*). Different cancers have varying sensitivities to treatment by radiation, and therefore some may be better suited to treatment by radioimmunotherapy. We have begun a trial to treat patients with lymphoma, a relatively radiosensitive tumor, using radiolabeled anti-B-cell monoclonal antibodies. Single radioiodinated antibody therapy doses are designed to deliver up to 1,500 rads to normal organs. This dose will be escalated in subsequent groups of patients until dose limiting toxicity is achieved. Doses are achieved by administration of as much as 600 mCi iodine-131- (^{131}I) labeled to anti-pan-B cell antibody. This paper details our methods for quantitative imaging and treatment of non-Hodgkin's lymphoma patients.

Specifically, we have treated patients with progressive B-cell lymphomas resistant to conventional therapy using radioiodinated antibody MB-1 (anti-CD-37) and 1F-5 (anti-CD-20). All patients were first studied with several escalating doses of trace-labeled anti-B-cell antibody to measure pharmacokinetics and estimate normal organ and tumor dosimetry. When a trace-labeled antibody dose showed favorable tumor-to-nontumor localization, the patient was treated using a single high dose of ^{131}I-antibody. With these high doses of ^{131}I, severe bone marrow toxicity was expected. In anticipation of this, all patients had their bone marrow aspirated and cryopreserved before treatment. Patients with severe marrow toxicity after treatment received autologous bone marrow transplantation. This paper describes the technical features of this study, including antibody radiolabeling, quantitative imaging and treatment, and summarizes our clinical results as validation of the importance of attention to methodologic detail in experimental radioimmunotherapy. The specific clinical results are detailed elsewhere (*6*).

METHODS and RESULTS

Antibodies

Anti-CD-37 B-cell antibody MB-1 (IDEC Pharmaceutical Corp., Mountain View, CA) is an IgG1 antibody recognizing a 40,000 dalton antigen present on virtually all human B-cells and 90% of human B-cell lymphomas (*7*). Crude antibody supernatant was produced in hollow fiber bioreactors and purified using both ammonium sulfate precipitation and ion exchange chromatography. The MB-1 preparation was 95% pure IgG, sterile, free of adventitious viruses, and passed general safety and endotoxin testing. Batches were prepared and administered to patients in accordance with a Notice of Claimed Investigational Exemption for a New Drug (B-IND 2510). Immunoperoxidase studies showed no cross reactivity

Received Jun. 26, 1989; revision accepted May 3, 1990.

For reprints contact: Janet F. Eary, MD, University of Washington Hospital, Division of Nuclear Medicine RC-70, 1959 Pacific St., Seattle, WA 98195.

with normal human kidney, liver, muscle, connective tissues, or other non-B-cell tissues. The CD-37 antigen was present in low concentration on other hematopoietic elements, however, including granulocytes and T-cells. An IgG2a anti-CD-20 B-cell antibody, 1F-5 (Oncogen Corp, Seattle, WA) that also recognizes human B-cells, was evaluated for biodistribution in two patients. A class-matched (either IgG1 if MB-1 was given, or IgG2a if IF-5 was given) murine anti-idiotype monoclonal antibody specific for another patient tumor (IDEC Pharmaceutical Corp., Mountain View, CA) was coadministered as a nonspecific antibody control. Several different nonspecific antibodies were used.

Radiolabeling

In a typical trace labeling for biodistribution measurement, 10 mg MB-1 antibody was reacted with iodination grade ^{131}I (nominally 7.7 Ci/mg from New England Nuclear, North Billerica, MA) to achieve a radiopharmaceutical specific activity of 1 mCi/mg. The chloramine-T method (*8,9*) was used and resulted in an average iodine/antibody molar ratio of 0.15. Using similar labeling methods, the nonspecific control antibody was iodinated with ^{125}I (nominally 17.4 Ci/mg, New England Nuclear, North Billerica, MA). After labeling, the radioimmunoconjugate was separated from free iodine by passing the reaction mixture over a 10-ml Sephadex G-10 column (Pharmacia Fine Pharmaceuticals, Uppsala, Sweden), previously washed with 10-column volumes of sterile isotonic saline. Fractions containing the labeled antibody were then combined, passed through a 0.22-μm sterilization filter, and aliquoted for final quality control testing. Each batch was evaluated for radiochemical purity using cellulose polyacetate electrophoresis at 300 V for 15 min with tris barbital buffer at pH 8.8 (Gelman Sciences, Ann Arbor, MI). Both the ^{125}I- and the ^{131}I-labeled antibodies showed >97% of the radioactivity present as protein bound material. Four to 10 mCi of ^{131}I were prepared for a total of 33 diagnostic labelings, and 2–5.2 mCi of ^{125}I were labeled for the same studies.

High-level labeling for radioimmunotherapy was performed by a variation of the method described by Ferens (*8*). The reaction took place in the shielded isotope shipping vial, which contained reductant-free high-specific activity ^{131}I. Labeling was performed in several batches with ~100 mCi of ^{131}I and 10 mg antibody for each labeling. Buffer, chloramine-T labeling reagents and antibody were introduced into the shipping vial through stainless steel needles connected to the reagent inlet. After mechanical agitation for 5 min, the reaction was terminated by addition of 12 μmole $Na_2S_2O_3$ quenching solution through the same needle. Any volatile iodine that may have developed during agitation was vented through a charcoal trap. Reaction products were withdrawn by means of a syringe connected to a new piece of i.v. tubing and transferred to the top of a preparative Sephadex G-10 column. The preparation was eluted with 0.05 *M* sterile phosphate-buffered saline. Labeled antibody eluted at the column bed volume. This fraction was collected separately and product yield was determined by assay in a dose calibrator (Capintec CRC-7, Pittsburgh, PA). To minimize product radiolysis, the sample volume was increased at least 10-fold using saline while quality control testing was performed (*10*). Quality control tests were performed as described above. Before administration, cold antibody was added to bring the total antibody content of the infused dose to the desired amount.

Five therapeutic labelings were performed (250, 482, 345, 232 mCi MB-1, 602 mCi 1F-5) with specific activities of 10 mCi/mg for MB-1 antibody, and 5 mCi/mg for 1F-5 antibody. Labeling yields assayed by cellulose polyacetate electrophoresis were similar to those for diagnostic preparations. For all labelings a mean value for protein bound radioactivity was 96.5%.

Prior to patient use of each multigram antibody lot, a portion was labeled and immunoreactivity was evaluated by cell-binding assay (*11*) using the RAJI malignant B-cell tumor line. Both low- (1 mCi/mg) and high- (10 mCi/mg) specific activity iodinated antibody preparations were incubated with varying numbers of live antigen-positive and antigen-negative control target cells. Immunoreactivity was assessed as the percent of total radioactivity specifically bound to antigen-positive target cells by measuring activity remaining in the supernatant after centrifugation and by extrapolating to infinite antigen excess. Avidity of each labeled antibody used in the trial was quantitated by performance of a full Scatchard analysis (*11*), adjusting for the immunoreactivity of the preparation.

To minimize the time between labeling and patient administration, an abbreviated immunoreactivity assay was devised for individual labelings prior to infusion. The percentage of specifically bound ^{131}I-labeled antibody was determined using two target cell concentrations (generally 10^7 and 10^6 cells/ml) and compared to an ^{125}I-labeled preparation of the same antibody that was previously fully characterized. Acceptance criteria for the patient labelings were >80% of control binding at both cell concentrations. Assay using these conditions did not determine true immunoreactivity but was sufficient to detect changes in either immunoreactivity or avidity compared to the control preparation. For the specific antibody trace labeled with ^{131}I, the cell-binding assay was ≥80% of expected immunoreactivity for every trace-labeled dose of MB-1 and 1F-5 antibody. Cell-binding assays were also done on each 100-mCi lot labeled in a therapeutic dose. These lots also showed immunoreactivity >80% of expected values.

Pyrogenicity was tested by a quantitative endotoxin test (Limulus Amebocyte Lysate, Associates of Cape Cod, MA). Pyrogen content is determined by this method with an accuracy of ±0.025 ng/ml. The pyrogen content of a preparation could not exceed 0.5 ng/kg of patient body weight for patient infusion (*13*).

Patients

Patients selected for entry into the trial had low or intermediate grade B-cell lymphomas resistant to conventional chemotherapy (*6*) (Table 1). Tumor samples were shown to be reactive with the MB-1 or 1F-5 antibody. Patients received no systemic anti-lymphoma chemotherapy in the four weeks

TABLE 1
Lymphoma Patients

No. of patients	Lymphoma type	Tumor mass (g)
5	Follicular small-cleaved cell	75–2710 g
3	Diffuse, small-cleaved cell	200–2300 g
2	Follicular mixed	60– 300 g

prior to study and had normal renal and hepatic function (creatinine <2.0 mg/dl, bilirubin <1.5 mg/dl).

Less than 25% involvement of bone marrow with lymphoma (determined by histologic examination of a biopsy) was required, along with no other active medical problems and an expected survival of more than 30 days. In addition, disease was progressing at a slow enough rate to obtain reliable biodistribution information from several week-long trace-labeled antibody imaging studies. Patients were excluded if they had a history of allergies to mouse protein, the presence of human anti-mouse antibody as determined by ELISA in our laboratory, prior radiation to maximum tolerated levels for any normal organ, or the inability to give informed consent.

Studies were approved by the University of Washington Human Subjects and Radiation Safety review committees. Informed consent was detailed with respect to the risks, alternatives, and possible benefits of participation in the trial. In particular, the experimental nature of the trial was emphasized.

Trace-Labeled Antibody Doses

Iodine-131-labeled antibody was administered in a dose-escalation protocol going from 0.5 to 2.5 to 10 mg/kg (*14*, *15*). This antibody was co-administered with control ^{125}I-labeled nonspecific class-matched anti-idiotype antibody at 0.2 mg/kg. Two to 3 ml of blood were sampled at 24-hr intervals and urine was collected for the following week. Immediately after antibody infusion at each dose, and during the week following, the patient was imaged daily to collect quantitative biodistribution data for dosimetry estimates. Time-activity curves for the normal organs, tumor sites, blood, and urinary excretion were generated, from which organ residence times were calculated. These were necessary data parameters for entry into the internal dosimetry computer program.

Quantitative Imaging and Biodistribution Data Collection

Iodine-131 imaging was performed with a General Electric 400 AT large field of view camera interfaced with a dedicated ADAC 3300 computer. The camera was equipped with a high-energy collimator and set to acquire at a 20% window centered at the 364 keV ^{131}I photopeak. At each image time, a sealed bottle 5 × 9, 2-cm deep standard of ^{131}I (100–200 μCi) was counted at a fixed distance (30 cm set arbitrarily) as similar to patient body thickness from the camera face. This permitted ^{131}I decay corrections and corrections for any drift in camera sensitivity between counting times. Counting this standard also determined the camera efficiency in cpm/mCi. All camera data were computer stored on floppy disks.

Whole-body radioiodine retention was determined using a 3× 3-in. collimated sodium iodide crystal aimed at the patient 15 feet away. Anterior and posterior counts were obtained for calculation of their geometric mean. The isoresponse of this instrument for ^{131}I was within ±5% over the height and width of the body. At each counting time, both background and a count of the ^{131}I standard were obtained at the same distance. Counts in the standard were used to correct the whole-body counts for changes in instrument sensitivity and radioisotope decay.

Accurate determination of normal organ outlines for computer-stored regions of interest (ROIs) were obtained by imaging the patient with technetium-99m (^{99m}Tc) radiopharmaceuticals prior to antibody infusion. For these images, the camera was set at a 20% energy window centered over the 140 keV photopeak, using a low-energy all-purpose collimator. The liver was imaged in the anterior and posterior views following injection of 5 mCi ^{99m}Tc-sulfur colloid. The camera was positioned at a close but comfortable distance over the patient. Similarly, the lung and kidney outlines were visualized; the former after injecting 2 mCi ^{99m}Tc-macroaggregated albumin and the latter after 2 mCi ^{99m}Tc-DTPA. From these images, ROIs were selected and stored in the computer (Fig. 1). After the ROIs were established, the patient was marked for repositioning for subsequent ^{131}I images. In subsequent ^{131}I images, other organ uptake (stomach or liver) sometimes interfered with whole-organ regions. When this occurred, small fixed 10×10 pixel ROIs were used to generate time-activity curves that were corrected for background. In the lung and liver regions, background was chosen that subtracted body wall thickness. In the kidney region, an adjacent abdominal ROI was selected.

The amount of radioiodine in each organ was estimated from conjugate view imaging (*16*,*17*). Attenuation by the patient was measured directly by imaging an ^{131}I flood source in air and with the patient interposed. The resulting transmission image was used to quantitate regional attenuation of the body. Counts in each organ were corrected by the attenuation

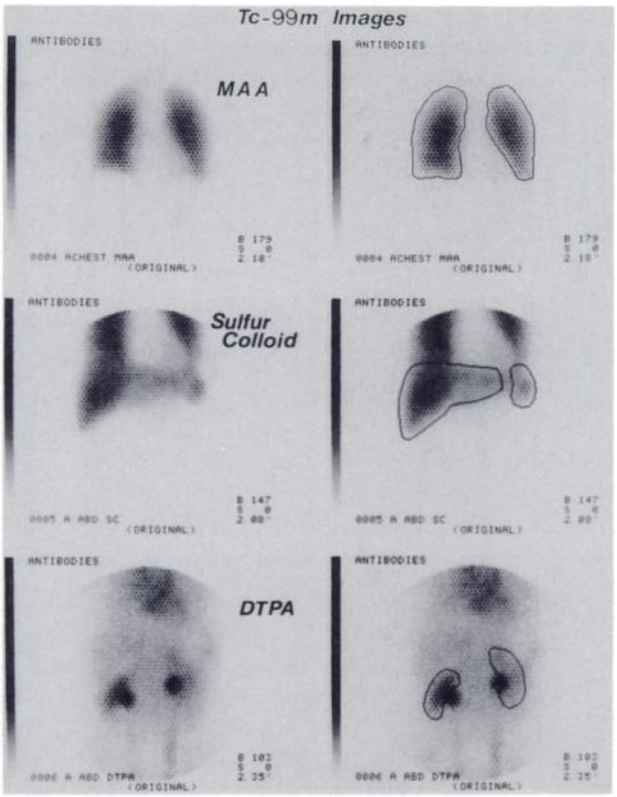

FIGURE 1
Images of normal organs using ^{99m}Tc agents. On the left are the unprocessed images, on the right are the same images with hand-drawn computer ROIs outlining the organs.

factor derived from the transmission image and were converted to microcuries by a camera sensitivity conversion factor (cpm/μCi). Total microcurie content in each organ was determined by the formula:

$$A = (I_a I_p)^{1/2} e^{(\mu_e T/2)} f/c,$$

where

A = activity (μCi).
I_a = cpm in anterior view.
I_p = cpm in posterior view.
μ_e = Effective linear attenuation coefficient, cm^{-1}, in each ROI, determined by flood source attenuation.
T = patient thickness (cm) in the ROI.
c = system calibration factor, (cpm/μCi).
f = self-attenuation correction for lesion thickness.

In our analysis of this equation and of data from phantom studies, the self-attenuation attributable to lesion thickness, f, was not different from that of the surrounding tissues. Consequently, it can be set to a value of 1 in the calculations without significantly affecting the calculation of A. Accordingly, a single attenuation factor derived from the ^{131}I flood source measurement in the ROI was used so that actual patient thickness was not measured. Quantitation of radioactivity in the normal organs is shown in Table 2.

We previously validated this method and showed it to be accurate to within ±6% for ^{131}I in a simple phantom model (*18*). In an anthropomorphic phantom with organs capable of being filled with radioactive liquids, and the body cavity filled with water, 1 mCi of homogeneously distributed ^{131}I in the liver cavity was quantitated with 4% error. When steps were taken to reduce scatter, either by asymmetric peak imaging, or use of a second collimator on top of the flood source, the error in the estimations was reduced to 2%. Five dogs were each given ~1 mCi ^{131}I, imaged by the above method, and then killed for absolute determination of radioactive content in organs by direct tissue counting. The percentage error in estimating ^{131}I content ranged from 0.2% to 2.9% in the major organs (liver, spleen, right kidney, and lung) (*18*).

Of the ten patients in this study, five showed tumor-positive images. Four (Patients 1, 2, 7, and 8) were positive with MB-1 and the other patient (#10) was positive with 1F-5 antibody

TABLE 2
Patient Organ and Tumor Uptake*

Patient	Infusion	Ab	Liver	Lung	Kidney	Spleen	Tumor	LI‡	Chest att†	Abd att†	Image result
1	1	MB-1	18.30	0.92	2.80	—	0.0058	11.8	2.06	3.26	+
	2	MB-1	17.00	6.90	2.99	—	0.0034	7.1			+
	3	MB-1	14.40	5.70	3.13	—	0.0035	15.0			+
2	1	MB-1	8.00	8.75	1.05	—			1.87	3.07	+
	2	MB-1	16.50	7.0	1.00	—	0.0015	4.8			+
	3	MB-1	16.60	5.30	0.90	—	0.0037	11.0			+
3	1	MB-1	19.80	2.45	0.20	—	0.0062	4.7	2.10	3.46	−
	2	MB-1	17.21	2.63	0.52	—	0.0004	2.8			−
	3	MB-1	18.47	4.63	0.70	—	0.0025	—			−
4	1	MB1	—	—	—	—	—	—	—	—	−
5	1	MB-1	21.99	8.52	0.90	8.55	0.00042	1.2	2.18	3.11	−
	2	MB-1	20.69	6.15	0.55	9.38	0.00078	1.01			−
6	1	MB-1	—	—	—	—	—				−
	2	MB-1	11.54	4.96	0.63	4.06	0.0021	2.1	1.93	3.05	−
7	1	MB-1	13.14	7.96	0.65	2.09	—	—			−
	2	MB-1	11.27	5.50	0.86	1.71	0.0054	7.4	1.77	2.39	+
8	1	MB-1	13.88	7.73	0.59	—	0.0014	1.75	1.60	2.19	+
	2	IF-5	11.21	5.97	0.53	2.61	0.0090	2.72			+
	3	MB-1	13.41	5.78	0.61	2.96	0.0022	1.0			+
9	1	MB-1	9.06	3.68	0.77	2.85	—	—	1.77	2.66	−
	2	MB-1	17.30	4.03	0.74	2.62	—	—			−
	3	IF-5	16.51	4.39	0.74	2.55	—	—			−
10	1	MB-1	10.61	4.06	0.56	3.34	0.0017	1.0	2.05	3.73	−
	2	MB-1	15.99	6.86	0.73	4.02	0.0017	1.3			−
	3	IF-5	11.75	4.74	0.53	2.86	0.0019	1.5			+
	Mean		16.17	5.32	1.04	3.97	0.0028	—	1.92	2.99	
	s.d.		3.16	12.12	0.84	2.79	0.0023	—	0.19	0.50	
	Total		23	23	23	13	18				

* Organ %ID determined immediately after antibody infusion by gamma camera imaging. Tumor uptake determined by biopsy at 48–72° postinfusion, %ID.

† Attenuation values determined from gamma camera transmission image.

‡ Localization index =

$$\frac{\text{tumor \% injected dose specific antibody/blood \% injected dose specific antibody}}{\text{tumor \% injected dose nonspecific antibody/blood \% injected dose nonspecific antibody}}.$$

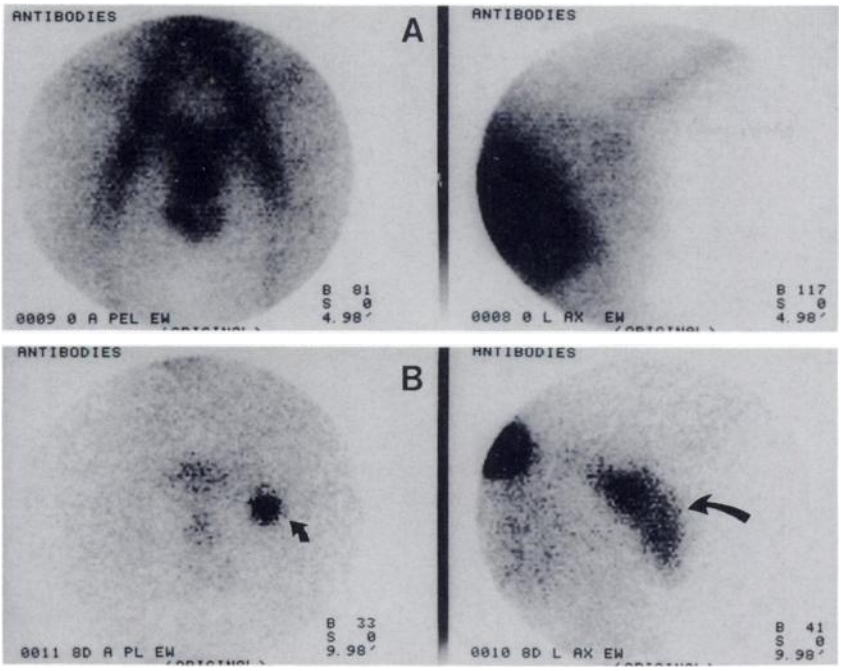

FIGURE 2
Images of the anterior pelvis (left) and left axilla (right) in Patient 1. (A) Images obtained immediately after infusion of 2.5 mg/kg ^{131}I-MB-1 antibody. (B) Images of the same areas 8 days after infusion. Arrows indicate lymphoma tumor masses.

(Table 2). In most cases, tumor was visible by 48 hr, and became distinct as background activity decreased during the week. Examples of patient images with distinct tumor localization are shown in Figures 2 and 3.

Patient tumors were biopsied 48–72 hr after radiopharmaceutical administration by CT-guided large bore needle or incision. Sections of tumor tissue in chilled RPMI tissue culture medium were counted for determination of radioiodine content. A multi-sample gamma counter (Packard Instruments, Downers Grove, IL) was set for dual-isotope counting with downscatter correction of ^{131}I (17%) applied to the counts in the ^{125}I window for each sample. A set of aliquoted dose standards was weighed and counted for each isotope for calculation of radioiodine concentration as a percentage of the injected dose/gram of tissue (%ID/g). Biopsies showed tumor uptake ranging from 0.0014% to 0.0090% of the ID/g in image-positive tumors (Table 2).

Serum and urine aliquots were counted in a similar manner. The %ID remaining in the plasma pool was determined by calculating the %ID/ml in a serum sample and estimating the plasma volume from a body surface area nomogram (*19*). Urinary excretion was reported as cumulative percent injected dose for each isotope, using the patient's report of time, date, and urine volume for each voiding. An example of cumulative urinary clearance is displayed in Figure 4.

Serum clearance of the diagnostic antibody doses always showed slower clearance with increased amounts of administered antibody. In all cases, the greatest dose of antibody

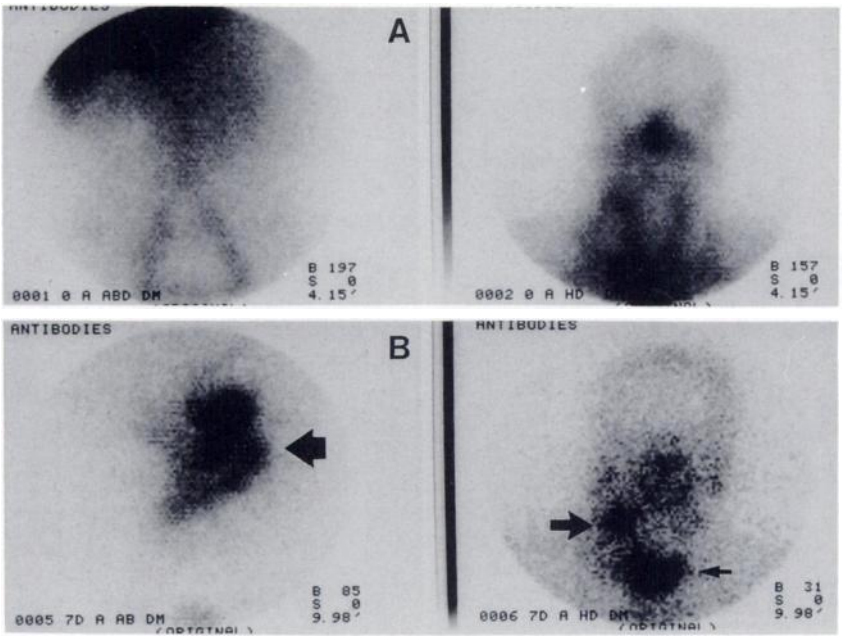

FIGURE 3
Images of Patient 2. The anterior abdomen is on the left and the anterior head is on the right. (A) Images obtained immediately after infusion of 10 mg/kg ^{131}I-MB-1 antibody. (B) On the left, antibody deposited in a large abdominal lymphoma mass (arrow), and on the right, antibody localization in a right neck lymphoma mass (large arrow) at 7 days after infusion. The small arrow denotes thyroid, which contained ~1% of the injected dose.

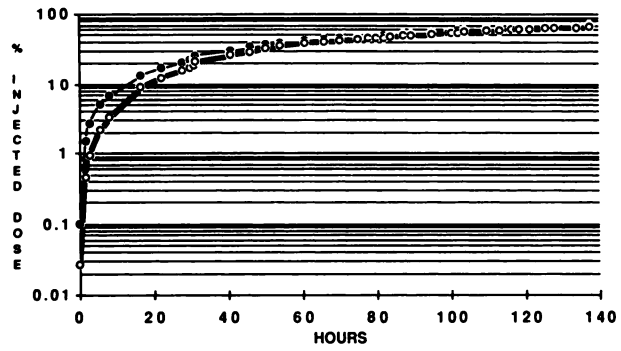

FIGURE 4
Cumulative percent injected dose in urine from 10 mg/kg in Patient 8. Solid circles are ^{131}I-labeled MB-1 antibody. Open circles are ^{125}I-labeled nonspecific antibody.

administered in image-positive patients showed a clearance half-time approaching that of the control antibody. An example of serum clearance data is shown in Figure 5. Serum and blood clearance were not different in spite of the fact that the antibody binds to circulating lymphocytes. The range of all serum clearance half-times is shown in Table 3. In all image-negative patients, clearance from the serum was rapid, and did not approach that of the control antibody. Clearance of radioiodine from the organs determined by imaging showed similar slowing of clearance with increasing amounts of antibody (Fig. 6). Table 3 also shows the range in clearance half-times obtained for all normal organs. Tumors were a special case in this set of data, showing slowing of clearance to a greater extent than the clearance from normal organs with greater antibody amounts. In most cases, the tumor clearance at the highest dose of antibody approached that of the decay half-time of ^{131}I (193 hr).

Tumor Histologic Examination

Because knowing the radiolabeled antibody content of tumor is critical to accurately estimating tumor radiation absorbed dose, biopsies of the patient's tumor at different antibody dose levels were examined microscopically for antigen

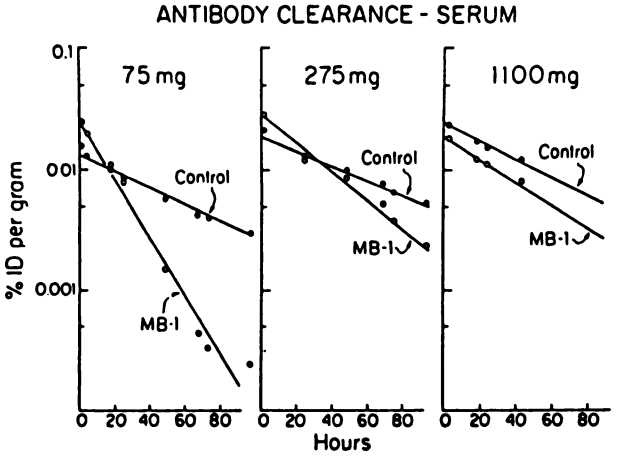

FIGURE 5
Serum antibody clearance at three doses of MB-1 (trace-labeled with ^{131}I) compared to simultaneously administered ^{125}I trace-labeled control antibody (Patient 1).

TABLE 3
Biologic Clearance $T_{½}$ (hr)

	0.5 mg/kg	2.5 mg/kg	10.0 mg/kg
Liver	11.5–19.1	17.5–29.1	11.1–39.9
Lung	12.4–14.3	20.4–32.8	33.4–67.9
Kidney	21.1–25.9	20.7–39.8	20.0–55.5
Spleen	9.6	12.6–32.8	35.3–94.9
Whole body	16.7–30.0	19.9–46.1	36.8–76.7
Serum			
Specific Ab	11.6–30.0	9.25–70.0	9.4–73.7
Nonspecific Ab	46.5–77.9	16.2–87.7	18.4–133.3

content, microscopic distribution of infused labeled antibody, and morphology. Tumor biopsy samples were fresh frozen, cut, and cold acetone fixed for analysis. Several sections were stained with hematoxylin and eosin to confirm that the biopsy contained viable tumor. These sections also allowed reconfirmation of tumor cell type and architecture (nodular versus diffuse lymphoma). Tumor-antigen content and distribution of infused murine antibody were evaluated by immunoperoxidase staining (*20*). MB-1 and IF-5 antibodies as the primary antibody were added directly to tissue sections to confirm the presence of antigen and assess antigenic distribution. This was particularly important in nodular lymphomas where internodular zones may have densities of antigen positive cells that vary by an order of magnitude. Sections were also reacted with a goat anti-mouse antibody for visualization of changes in distribution of the infused labeled murine tumor specific antibody (MB-1, IF-5), at different dose levels. Immunoperoxidase stained sections showed increased tumor penetration of antibody (beyond pericapillary areas) with increasing antibody dose. These dimensions are of the same magnitude as the range of beta particles from ^{131}I.

Estimating Radiation Absorbed Dose

The radioimmunotherapy protocol is designed such that groups of three patients receive the same escalating doses of radiation to normal organs. These dose steps are intended to determine the toxicity of this experimental treatment for non-Hodgkins lymphoma. Because we expect to approach the limit of normal tissue toxicity from radiation delivered by antibodies, we carefully estimate the radiation absorbed dose to critical normal organs as well as tumor.

Each therapy dose is tailored to the individual patient, making the use of the organ volumes of the standard MIRD man inappropriate. At the time of the imaging study, estimates of tumor and organ volumes (liver, lung, spleen, and kidneys) were obtained by CT imaging from the trunk to the pelvis at slice intervals of 1 cm. In each slice, the organ or tumor contour was outlined. The organ and tumor volumes were then estimated by multiplying the surface area of the organ contour by the thickness of the slice. The volumes of those slices were summed to determine total organ volume. By current methods, using contour outlining software for irregularly shaped objects, the accuracy of these calculations are estimated to be ±5% (*21*).

A full set of biodistribution data was obtained for each antibody trace-labeled dose. Time-activity curves were carefully inspected and fit by least-square's regression to derive

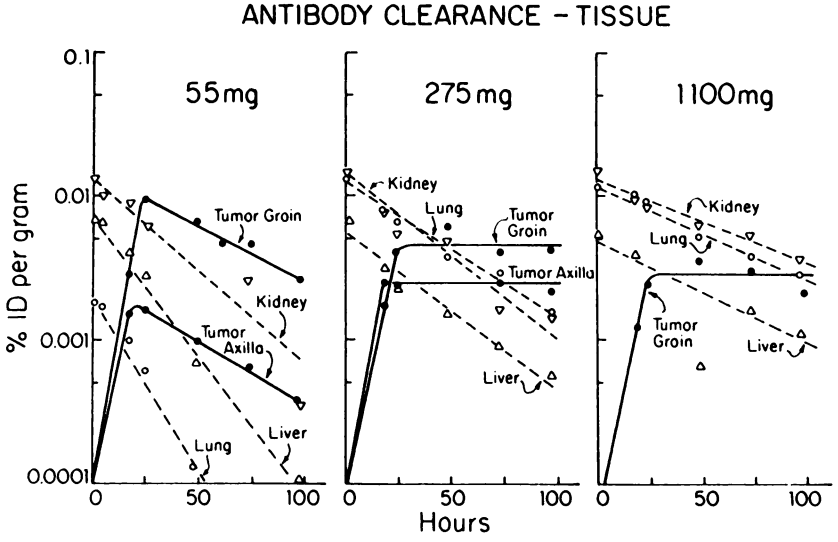

FIGURE 6
Clearance of ^{131}I-labeled MB-1 antibody from normal organs and tumors in Patient 1. Data derived from gamma camera imaging.

estimates for effective clearance half-times of the radionuclide in the tissues. These were used to estimate cumulated activities for the major source organs. Uptake data for tumor included values derived from biopsy at 48–72 hr postinfusion as well as values determined by imaging.

The method used for calculating the absorbed dose from ^{131}I was based on the MIRD system for internal dosimetry, which took into account cross-organ photon absorption, irregular shapes of organs, increased density of bone, and the build-up factor for secondary ionization (*22–23*). Organ weights for MIRD calculations were adjusted for each patient according to the CT-derived measurements. The computer software MIRDOSE (Internal Dose Information Center at Oak Ridge Associated Universities, Oak Ridge, TN) was used for selected source organs and desired target organs. Data output was reported in units of rads/mCi injected for each of the major target organs and also included a whole-body dose estimate.

Absorbed dose estimates are shown in Table 4. Single high-dose ^{131}I antibody preparations for therapy were given to the patients in whom diagnostic doses predicted that the tumor would receive radiation absorbed dose (rads/mCi) equal to or greater than that in any normal organ excluding bone marrow. In three patients (#1, #2, and #7), therapeutic doses based on these estimations were calculated to deliver ≤1,000 rad to any normal organ, with higher doses delivered to tumors. In two other patients (#8 and #10), the highest dose to a normal organ was escalated to ~1,500 rad. Tumor therapeutic doses ranged from 850 to 4260 rad/tumor mass.

TABLE 4
Absorbed Dose Estimates for Therapeutic Infusions (rads)

	Patient				
	1	2	7	8	10
	(250 mCi)	(482 mCi)	(345 mCi)	(232 mCi)	(602 mCi)
Site	MB-1	MB-1	MB-1	MB-1	1F5
Tumor #1	850	4260	1180	1830	1678
Tumor #2	1300	930	1330	—	—
Liver	380	858	560	730	945
Kidney	700	606	540	630	775
Lung	650	990	1080	1570	1600
Spleen	—	—	1100	1930	2371
Whole body	100	253	150	240	344

Antibody clearance data collected after the therapy doses confirmed that the trace-labeled doses had accurately predicted the behavior of the therapy dose. An example of this data is shown in Figure 7, which compares serum clearance data from a trace-labeled dose to the therapy dose for patient 10.

Radiopharmaceutical Infusion

Before infusion of each radiopharmaceutical dose, a serum sample was assayed for the presence of human anti-mouse antibody (HAMA) using an enzyme-linked immunoadsorbent assay. One patient in this group developed HAMA after four serial infusions of antibody.

Eight patients had a large bore right atrial catheter (Hickman type) placed for blood sampling and administration of medication, including, if required, bone marrow reinfusion. The central line facilitated frequent accurately timed blood sample withdrawal. In all cases, the lines were well tolerated. Patients were pre-treated with oral Tylenol (650 mg acetaminophen), Lugol's iodine solution (3–5 drops daily), 25–30 mg diphenhydramine (1 mg/ml), and 110 mg hydrocortisone, intravenously. In addition to these medications, epinephrine (1 mg/ml) and a standard hospital emergency cart were always accessible during the infusion period (up to 4 hr) and in the 2-hr interval postinfusion.

Antibody infusion took place in the gamma camera imaging suite, where patients were lying supine on the imaging table or sitting upright in a recliner designed for chemotherapy infusion. A separate i.v. line was placed for antibody infusion. Imaging doses were infused at a rate of 250 mg/hr. During antibody infusion, the patient was under direct observation by a physician, with vital signs monitored every 30 min, or more frequently if adverse reactions developed. In the event of an adverse reaction (fever, hypotension, urticaria), antibody administration was stopped, with re-administration of i.v. diphenhydramine. When the adverse reaction subsided, antibody administration was resumed at a slower rate. At completion of antibody administration, the infusion line was flushed with normal saline and removed.

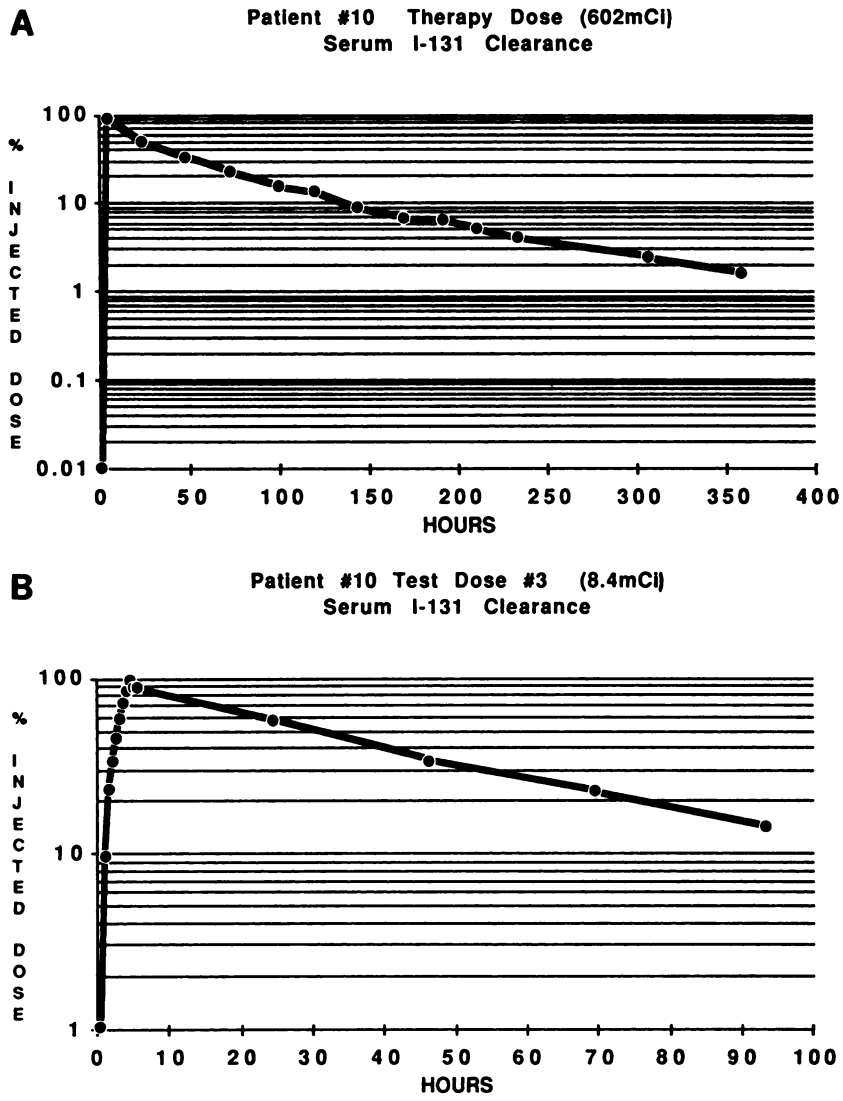

FIGURE 7
(A) Serum clearance of trace-labeled dose of 2.5 mg/kg IF5, with a clearance half-time of 30 hr. (B) Serum clearance of the therapy dose. Clearance half-time was 30 hr.

Ten patients were studied in the dose-escalation protocol (Table 2). Patient 4 left the study after one infusion of MB-1 (2.5 mg/kg) because of marked thrombocytopenia (platelets falling from 100,000 to 13,000/mm^3) 24 hr after infusion. Other mild reversible acute toxicities were sometimes encountered during diagnostic antibody infusion. Three patients experienced low-grade fever, three developed urticarial rashes, three developed myalgias, two experienced mild throat tightness, and one patient developed mild hypotension which resolved rapidly with saline infusion.

All were successfully treated with additional diphenhydramine, acetominophen, and hydrocortisone for resolution of symptoms that allowed completion of the antibody infusion. Three patients experienced recurrent urticaria 5–6 hr after infusion, which was treated successfully with additional oral diphenhydramine. These mild reactions were easily treated, but gave ample evidence that the investigating nuclear physician needed to be prepared to treat severe life-threatening adverse reactions.

Therapeutic Infusions

Patients received the therapeutic dose in an isolated room on the oncology floor of the University of Washington Medical Center. The room was prepared with collection containers for linen and waste and the patient's bed was shielded with portable brachytherapy shields. Patients were instructed in self-care techniques, which included monitoring vital signs, blood sample withdrawal from the Hickman line, and recording fluid intake and output measurements. The therapeutic dose of radiopharmaceutical was placed in an i.v. solution bag in a heavily shielded portable lead container and was infused using a peristaltic pump (Abbott/Shaw Lifecare Pump Model 4, North Chicago, IL) set to deliver the dose at a rate of 250 mg antibody/hr. During infusion, the patient monitored his own vital signs and withdrew blood samples for biodistribution evaluation according to schedule and at the request of the physician. This served to reduce contact between the patient and attending personnel. Physicians remained in the hospital corridor within direct sight of the patient throughout the entire infusion and postinfusion period. They and other personnel closely monitored the dose infusion set-up and patient during this time. Personnel attending the patient wore dosimeters which emitted audible warnings (Xetex model 4158, Xetex, Inc. Mountain View, CA).

At the termination of infusion, the Radiation Safety Officer monitored the room using a portable survey meter to map

exposure rates in mR/hr in the patient's room and surrounding areas. This map was posted on the door of the patient's room, along with appropriate radiation warning signs. This exposure rate information was used to determine the adequacy of shielding. Safe lengths of time for visits at the doorway by hospital personnel, family members, and visitors were established, which were typically 20 min. The Radiation Safety Officer monitored the patient on a daily basis and informed the investigators when the total-body radioactive burden dropped below 30 mCi, typically on the 7th to 10th day after administration. Then the patient was discharged. All personnel involved with the therapy were monitored for thyroid radioiodine content.

After hospital discharge, the patients were followed as outpatients and gamma camera images were obtained. During the study, and in the post-therapy period, patients had complete blood cell counts with platelet counts three times a week. Serum electrolytes, creatinine, blood urea nitrogen, and liver function tests were ordered at the same intervals. Variations in normal B-cell populations were determined by correcting the absolute lymphocyte count by the percent of circulating lymphocytes reactive with anti-CD-20 antibody using flow cytometry. Patient tumor masses were monitored by CT or MRI 1 wk and 3 mo post-therapy and were compared to pre-study images. Thyroid function studies were obtained before and 3, 6, and 12 mo after therapy.

Five patients with tumor-positive images received therapeutic radiolabeled antibody doses. None had immediate toxicity (*6*). Lack of toxicity from these infusions was a result of specific medication and an antibody infusion rate designed for each patient, based on the adverse reaction the patient experienced from the diagnostic infusions prior to treatment. For example, if the patient required prednisone and repeated doses of i.v. diphenhydramine during the diagnostic infusions, then those medications were administered at the outset of the treatment infusion and on the same schedule during the therapeutic infusion period.

Monitoring immediately after infusion showed exposure rates of 24 to 100 mR/hr at one meter from the patient. Survey of the room after discharge of the patients detected contamination of the linen, undergarments, and disposable eating utensils. Room fixtures and furniture were not ordinarily contaminated, with the exception of a few surfaces which were repeatedly handled by the patient receiving the highest dose. Radiation exposure to the investigator ranged from 3 to 7 mR per patient therapy. There were no radiation safety problems encountered in transporting or administering the therapeutic doses of radiolabeled antibodies or in waste disposal.

Post-therapy imaging showed antibody localization of therapeutic dose in tumors. Figure 8 shows an image of Patient 10, 13 days after treatment; it was comparable to the diagnostic images. For the first few days after a therapy dose, high count rate paralyzed the camera so that early tumor and normal organ clearance of the therapy doses could not be determined.

Four of the five patients that were treated experienced complete tumor remissions (*6*). Patient 10 had a partial response. In these responses, tumor sizes decreased to normal lymph node size or were undetectable by CT scan 3–4 wk post-therapy. Patients receiving 1,000 rad to a normal organ experienced significant bone marrow toxicity and required platelet support during the period of severe cytopenia. Peripheral blood counts decreased over a period of 3 wk, with the nadir occurring in the fourth week (Fig. 9). During this period of severe cytopenia, none of the patients had life-threatening infections or other problems. Bone marrow function spontaneously recovered 2–3 wk after the nadir in peripheral counts, being heralded by stability of platelet counts after transfusion. The two patients receiving the highest dose (1,500 rad) to the normal organs were given their previously stored bone marrow because of severe prolonged pancytopenia. In 2–3 wk, these patients recovered normal marrow function and experienced no complications (Fig. 9). Long-term toxicities were observed in the thyroid function of Patients 1 and 2, who became hypothyroid one year after treatment. To date none of the other patients have shown hypothyroidism. Careful monitoring of radiation toxicity signs has been essential in helping the investigators calibrate the accuracy of dosimetry estimates.

DISCUSSION

The first goal of this project was to carefully determine the pharmacokinetics of radiolabeled anti-lymphoma antibodies in each patient to understand and formulate antibody dose scheduling protocols. In addition, there was the goal of accurate dosimetric estimation for high-dose ^{131}I treatment. A final goal was to establish toxicity and efficacy of single high-dose radioimmunotherapy administrations. All of these objectives presented significant challenges to the nuclear medicine group. The role that nuclear imaging and data gathering

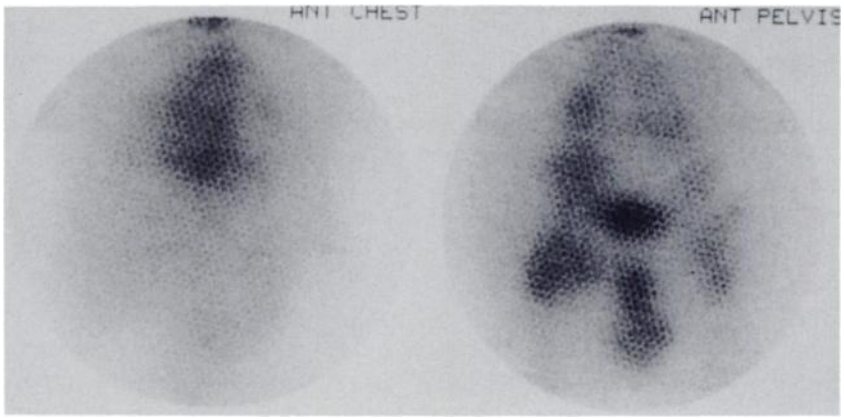

FIGURE 8
Images of the anterior chest (left) and anterior pelvis (right) of Patient 10 obtained 6 days after the infusion of the 602 mCi ^{131}I-IF-5 antibody therapeutic dose (10 mg/kg). The pelvis image shows localization of the therapeutic antibody dose in lymphoma masses in the inguinal regions and iliac groups bilaterally.

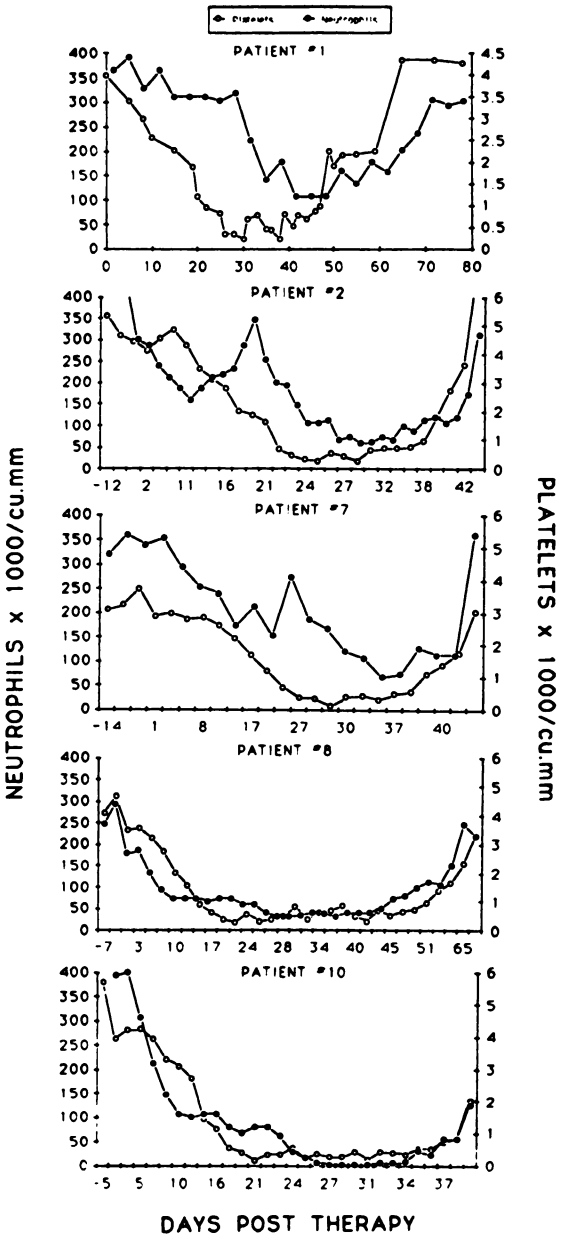

FIGURE 9
Peripheral blood counts post-therapy in treated patients. Patients 8 and 10 required infusion of previously stored bone marrow which engrafted successfully.

plays is evident in the detailed description presented in the Methods/Results section.

In this report, we have described production of a reproducible and high quality antibody radiopharmaceutical, as well as quality control methods, that we believe are necessary to ensure safe procedures as well as interpretable results. Confidence that the radiopharmaceutical maintains high quality cannot be overly emphasized; this enabled us to be certain that our pharmacokinetic studies on these patients had validity with respect to development of strategies for choice of antibody and dosing schedules. Similarly, rigorous examination of radiopharmaceuticals used for the therapeutic administrations gave us confidence that the kinetics of the therapeutic dose followed that of the trace labeled antibody in the preliminary study. This was confirmed by the blood clearance data and images obtained several days after administration.

Acquisition of biodistribution data by gamma camera imaging also underscored the importance of consistency and quality control in imaging. The time-activity data acquired from each of the studies provided data from which to make observations about the behavior of each antibody dose and/or antibody in each patient. While there are known limitations to quantitative planar imaging, it is a simple technique which yielded consistent, reasonable results in our hands. We are currently involved in studies to further validate the method using simple and complex anthropomorphic phantoms.

In this study of patients in whom it was possible to image sites of tumor, dosimetric estimations qualified them for treatment. Tumors were well visualized by 48 hr and required no image enhancement or background subtraction techniques to improve detectability. Superficial and deep-seated tumors were equally well visualized, in contrast to other reports (*25*). Because of the clear visualization of these masses, it was possible to generate accurate time-activity curves, which are the largest source of error in estimation of tumor dosimetry. Combination of these curves with uptake data obtained by direct tumor biopsy provided input data for estimations of tumor absorbed dose for treatment planning. This is in contrast to radioimmunotherapy protocols by other groups where dose escalation is based on mCi/kg, or mCi radioactivity, without regard to estimation of radiation absorbed dose delivered by the treatment. We have seen in this patient series that organ and tumor radiodine residence times vary significantly between patients at the same antibody dose. This would necessarily lead to markedly different radiation absorbed doses to these sites if the radioactivity for therapy had been administered on a millicurie basis. If our protocol had been designed in this way, patients would have received suboptimal tumor absorbed radiation doses. In addition, normal organ toxicity inferred from cumulative rads of exposure would have been unpredictable.

The methods described here provide a detailed study of each individual patient at each antibody dose. A great deal of effort was expended to minimize the assumptions for calculation of radiation absorbed dose for each patient. Time-activity curves were acquired for each normal organ and tumor. Whole-body CT scans allowed use of actual patient organ volumes in the MIRDOSE formulation, rather than using the standard 70-kg MIRD-MAN assumption. The gain of this study design was in understanding how pharmacokinetic and

biodistribution factors interact in radioimmunotherapy. This resulted from extensively using the patient as his own control by performing serial studies with different antibody doses.

The therapeutic doses used were high but were given safely in the hospital environment with acceptable levels of radiation exposure to the investigator, laboratory, and nursing personnel. This was, in large part, due to careful planning and utilization of a remote labeling set-up, as well as adequate shielding of the dose and treated patient and allowing the patient to do certain aspects of his own care.

The results of treatment of these patients showed that the dosimetric estimations obtained by our methods were good predictors of toxicity and efficacy. We have not observed radiation toxicities in the lung, liver or kidney; we predicted severe marrow toxicity without normal organ toxicity and have observed complete tumor regression with this level of bone marrow toxicity. Acute exposure to a whole-body radiation dose of <400 rad sterilizes the bone marrow (*26*), leading us to predict that the patients receiving the higher whole-body doses would have severe pancytopenias. The two patients receiving the higher radiation doses required autologous bone marrow rescue. It is not clear from the time of recovery of blood counts whether patients had bone marrow engraftment, spontaneous recovery or both. We believe that the whole-body dose is a better predictor of bone marrow toxicity than a calculated bone marrow dose. The isotope uptake and residence time in the bone marrow is difficult to ascertain with confidence. Gamma camera imaging methods observing major sites of bone marrow can be inaccurate due to interference from overlying major blood vessels (sacroiliac joints, vertebral column). The iliac wings in our patients who have had previously stored marrow are scarred and remodeling. This also precluded our obtaining accurate direct marrow uptake data by biopsy. Current models of bone marrow dosimetry based on circulating blood radioactive concentrations are fraught with inconsistencies and questionable assumptions regarding bone marrow mass and blood flow exchange rates with peripheral blood. For these reasons, whole-body dose estimations based on cross-organ doses derived from the MIRD formulations will be better predictors of bone marrow toxicity. At this time, we still do not have plans in this study protocol to calculate bone marrow doses derived from primary biodistribution data. The need for autologous marrow rescue may also depend on the amount and type of previous chemotherapy.

In summary, this report details our methods for evaluating lymphoma patients for radioimmunotherapy, while pursuing the larger goal of understanding radiolabeled anti-tumor antibody pharmacokinetics. These studies continue, supported by efforts directed toward developing and validating improved methods for radiolabeling and quantitative imaging validation, and dosimetry estimations, to account for heterogeneous distribution of ^{131}I within tumor.

ACKNOWLEDGMENTS

Supported by NIH Grants #CA44991 and CA47430.

REFERENCES

1. Horowitz JA, Goldenberg DM, DeJager R, et al. Phase I/II trial of radioimmunotherapy (RAIT) with I-131 labeled anti-CEA and anti-AFP monoclonal antibodies. *J Nucl Med* 1988; 29:846.
2. Rosen SA, Zimmer A, Goldman-Leiken R, et al. Radioimmunodetection and radioimmunotherapy of cutaneous T-cell lymphomas using an I-131 labeled monoclonal antibody: an Illinois Cancer Council study. *J Clin Oncol* 1987; 5:562–573.
3. Order S, Stilwagon G, Klees J, et al. Iodine I-131 anti-ferritin, a new treatment modality in hepatoma: a radiation therapy oncology group study. *J Clin Oncol* 1985; 3:1573–1582.
4. DeNardo S, DeNardo G, O'Grady L, et al. Pilot studies of radioimmunotherapy of B-cell lymphoma and leukemia using I-131 Lym-1 monoclonal antibody. *Abs Immunoconj Radiopharm* 1988; 1:17–33.
5. Carrasquillo JA, Krohn KA, Beaumier PL, et al. Diagnosis of and therapy for solid tumors using radiolabeled antibodies and immune fragments. *Cancer Treat Rep* 1984; 68:317–328.
6. Press OW, Eary JF, Badger CC, et al. Treatment of refractory non-Hodgkin's lymphoma with radiolabeled MB-1 (anti-CD37) antibody. *J Clin Oncol* 1989; 7:1027–1038.
7. Link M, Bindle J, Meeker T, et al. A unique antigen on mature B-cells defined by a monoclonal antibody. *J Immunol* 1986; 37:3013–3018.
8. Ferens JM, Krohn KA, Beaumier PL, et al. High level iodination of monoclonal antibody fragments for radiotherapy. *J Nucl Med* 1984; 25:367–370.
9. Hunter WM, Greenwood FC. Preparation of I-131 labeled human growth hormone of high specific radioactivity. *Nature* 1962; 194:495.
10. Kishore R, Eary J, Krohn KA, et al. Autoradiolysis of iodinated monoclonal antibody preparations. *Int J Nucl Med Biol* 1986; 13:457–459.
11. Lindmo T, Bouen E, Cuttita F, et al. Determination of the immunoreactive fraction of radiolabeled antibody by linear extrapolation to binding at infinite antigen excess. *J Immunol Meth* 1984; 72:77–79.
12. Scatchard G. The attraction of proteins for small molecules and ions. *Ann NY Acad Sci* 1949; 51:660.
13. Cohen J, McConnell JS. Observations on the measurement and evaluation of endotoxemia by a quantitative limulus lysate assay. *J Infect Dis* 1984; 150:916–924.
14. Badger CC, Krohn KA, Shulman H, et al. Experimental radioimmunotherapy of murine lymphoma with I-131 labeled anti-T-cell antibodies. *Cancer Res* 1986; 46:6223–6228.
15. Badger CC, Krohn KA, Peterson A, et al. Experimental radiotherapy of murine lymphoma with I-131 labeled anti-Thy 1.1 monoclonal antibody. *Cancer Res* 1985; 45:1536–1544.
16. Hammond ND, Moldofsky PJ, Beardsley MR, et al. External imaging techniques for quantitation of distribution of I-131 $F(ab')_2$ fragment of monoclonal antibody in humans. *Med Phys* 1984; 11:778–783.
17. Thomas SR, Maxon HR, Kereikes JG, et al. Quantitative external counting techniques enabling improved diagnostic

and therapeutic decisions in patients with well-differentiated thyroid cancer. *Radiology* 1972; 122:731–737.
18. Eary JF, Appelbaum FL, Durack L, et al. Preliminary validation of the opposing view method for quantitative gamma camera imaging. *Med Phys* 1989; 16(3):382–387.
19. Hurley PJ. Red cell and plasma volumes in normal adults. *J Nucl Med* 1974; 16:46–52.
20. Sternberger LA, Hardy PH, Cuclis JJ, et al. The unlabeled antibody enzyme method of immunohistochemistry. Preparation and properties of soluble antigen-antibody complex (horseradish peroxidase-antihorseradish peroxidase) and its use in the identification of spirochetes. *J Histochem Cytochem* 1970; 18:315–333.
21. Heyersfeld SB, Fulenweider T, Nordlinger B, et al. Accurate measurement of liver, kidney and spleen volume and mass by computerized axial tomography. *Ann Intern Med* 1979; 90:185–187.
22. Snyder WS, Ford MR, Warner GG, et al. "S" absorbed dose-per unit cumulated activity for selected radionuclides and organs. *MIRD pamphlet No. 11.* New York: Society of Nuclear Medicine; 1975.
23. Loevinger R, Berman M. A revised schema for calculating the absorbed dose from biologically distributed radionuclides. *MIRD pamphlet No. 1.* New York: Society of Nuclear Medicine; 1976.
24. Press O, Appelbaum F, Ledbetter J, et al. Monoclonal antibody IF5 (anti-CD-20) serotherapy of human B-cell lymphomas. *Blood* 1987; 69:584–591.
25. Carrasquillo JA, Mulshin JL, Bunn PA, et al. Indium-111-T101 monoclonal antibody is superior to iodine-131-T101 in imaging of cutaneous T-cell lymphoma. *J Nucl Med* 1987; 28:281–287.
26. Vriesendorp HM, Van Bekkum DW. Susceptibility to total body irradiation. In: Broerse JJ, MacVittie T, eds. *Response to total body irradiation in different species.* Amsterdam: Martinius Nijko; 1984.